Journal of Alloys and Compounds 509 (2011) 7066–7070

Contents lists available at ScienceDirect

Journal of Alloys and Compounds

journal homepage: www.elsevier.com/locate/jallcom

Enhanced microwave absorption properties of $Fe_{73.5}Cu_1Nb_3Si_{15.5}B_7$ nanoflakes by moderate surface oxidization and rotational orientation in composites

Weifeng Yang, Liang Qiao, Tao Wang*, Fashen Li*

Institute of Applied Magnetics, Key Laboratory for Magnetism and Magnetic Materials of Ministry of Education, Lanzhou University, Lanzhou 730000, People's Republic of China

ARTICLE INFO

Article history:
Received 8 July 2010
Received in revised form 29 March 2011
Accepted 30 March 2011
Available online 6 April 2011

PACS:
75.50.Bb
72.30.+q
72.80.Tm
77.22.Ch

Keywords:
FeCuNbSiB
Nanoflake
Moderate oxidization
Rotational orientation
Microwave absorption

ABSTRACT

$Fe_{73.5}Cu_1Nb_3Si_{15.5}B_7$ nanoflakes were fabricated by ball milling the annealed ribbons. The microwave absorption properties of $Fe_{73.5}Cu_1Nb_3Si_{15.5}B_7$ nanoflakes were improved by moderate surface oxidization and rotational orientation in composites. As for the oxide-coated nanoflakes composite, the permittivity decreased distinctly and the permeability maintained the initial value compared with the as-milled nanoflakes composite. Through rotational orientation, the lower permittivity and higher permeability were obtained, and consequently the microwave absorption properties were improved obviously. The minimum reflectivity for the absorber of the oriented composites with 35 vol% oxide-coated nanoflakes could reach −46.4 dB at 1.31 GHz with the thickness of 4.2 mm.

1. Introduction

With the rapid development of microwave technology, the microwave absorbing materials (MAMs) have been applied widely in many fields, such as electromagnetic shielding, stealth defense and wireless communication. Metallic magnetic materials, especially Fe-based alloys, have demonstrated excellent microwave absorption properties [1–5]. Among the Fe-based alloys, FeCuNbSiB alloy is a kind of preferable soft magnetic materials with high saturation magnetization, high permeability, and low coercivity [6]. However, the applications of FeCuNbSiB in microwave absorption are relatively scarce. Therefore, it's of significance to explore its potential applications in the field of microwave absorption.

The high permeability and low reflectivity in higher frequency range are required in the applications of MAMs. The flake-shaped particles have advantages in increasing high-frequency permeability and resonance frequency simultaneously according to the bianisotropy picture [7]. However, the impedance matching between materials and free space must be paid more attention, which requires the permeability equal to the permittivity [8]. For most metallic magnetic materials, the permittivity is much larger than the permeability [9–12]. Therefore, it's important to enhance their microwave absorption properties by decreasing the permittivity and increasing the permeability. For the sake of decreasing permittivity, the oxide-coating on the surface of the particles is necessary to suppress the polarization of electric charge and decrease the permittivity effectively [13]. In order to further increase the permeability, the rotational orientation for the composite is extremely effective by making the easy direction of magnetization of the nanoflakes located in the orientation plane [14]. The above mentioned two methods can improve the impedance matching and enhance the microwave absorption properties of MRMs.

In this study, $Fe_{73.5}Cu_1Nb_3Si_{15.5}B_7$ nanoflakes were fabricated by ball milling the annealed ribbons. Then, a thin oxide-shell was coated on the nanoflakes by moderate oxidization in a hydrogen peroxide solution. Furthermore, the oxide-coated nanoflakes were embedded in paraffin wax with rotational orientation in an external magnetic field. The as-milled nanoflakes composite, the oxide-coated nanoflakes composite and its oriented composite were measured in the frequency range of 0.1–18 GHz. Their microwave absorption properties were investigated for the absorber's thicknesses of 1.0–8.0 mm.

* Corresponding authors. Tel.: +86 931 8910801; fax: +86 931 8910801.
E-mail addresses: wangtlz@hotmail.com (T. Wang), lifs@lzu.edu.cn (F. Li).

0925-8388/$ – see front matter © 2011 Elsevier B.V. All rights reserved.
doi:10.1016/j.jallcom.2011.03.168

2. Experimental details

2.1. Preparation

In this study, the amorphous $Fe_{73.5}Cu_1Nb_3Si_{15.5}B_7$ ribbons were annealed in a vacuum furnace at 540 °C for 1 h and then milled for 12 h using a vibrating ball mill with the ball-to-powder weight ratio of 20:1 in absolute ethyl alcohol. The annealed ribbons became brittle and easier to be milled into micron-sized particles compared with their amorphous state. In order to coat the particles with a thin oxide-shell, it's feasible to employ a weak but moderate oxidization reaction occurring on the surface of particles. We added the as-milled powder (0.5 g) into the mixture of hydrogen peroxide (30% solution) (10 ml) and anhydrous alcohol (10 ml) under an ultrasonic action of 450 W for 3 h, and then the powder was naturally dried in room temperature. The composites were prepared by putting the powder (0.20 g) embedded in the paraffin wax (0.04 g) and pressing the mixture into toroidal shape (out diameter φ_{out}: 7.00 mm, in diameter φ_{in}: 3.04 mm, and thickness d: ~2 mm). The volume concentration of the powder in composite is about 35%. The oriented composite was fabricated with a rotational orientation method described in our previous study [14]. For convenience, the as-milled powder was marked as Sample A and the oxide-coated powder was marked as Sample B. Accordingly, the composite of Sample A was denoted as Composite A and the composite of Sample B was denoted as Composite B. The oriented composite of Sample B was denoted as Composite C. The experimental procedure is shown in Fig. 1.

2.2. Characterization

The morphology and size distribution of the particles were analyzed by scanning electron microscope (Hitachi S-4800) and transmission electron microscope (JEM 1200EX). The phase and composition analysis were carried out by powder X-ray diffractometer (Philips X'Pert) with Cu Kα radiation and X-ray photoelectron spectrometer (ESCALAB 210) with Mg Kα radiation, respectively. The magnetic properties of the samples were measured using a vibrating sample magnetometer (Lakeshore 7304 model). The relative complex permittivity ($\varepsilon_r = \varepsilon' - j\varepsilon''$) and complex permeability ($\mu_r = \mu' - j\mu''$) were determined from the scattering parameters measured on the composites with 35 vol% powder by a vector network analyzer (Agilent E8363B) in the frequency range of 0.1–18 GHz. The frequency dependence of reflectivity R was calculated with the measured relative complex permittivity and permeability by the following equations [15]:

$$R = 20 \log \left| \frac{Z_{in} - Z_0}{Z_{in} + Z_0} \right|, \quad (1)$$

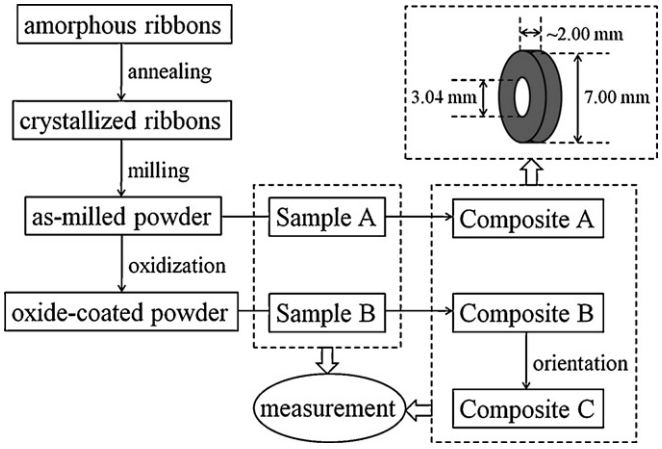

Fig. 1. The schematic diagram of the experimental procedure.

$$Z_{in} = Z_0 \sqrt{\frac{\mu_r}{\varepsilon_r}} \tanh \left[j \left(\frac{2\pi f t}{c} \right) \sqrt{\mu_r \varepsilon_r} \right], \quad (2)$$

$$Z_0 = \sqrt{\frac{\mu_0}{\varepsilon_0}}, \quad (3)$$

where Z_0 is the impedance of free space, Z_{in} is the input impedance of the absorber, μ_r and ε_r are the measured relative complex permittivity and permeability, respectively, μ_0 and ε_0 are permeability and permittivity of free space, c is the light velocity (3×10^8 m/s), and t is the thickness of the composite absorber. The minimum reflectivity R_{min} was defined as the minimum value of R with a certain thickness in the frequency range of 0.1–18 GHz [16]. The bandwidth Δf at different thicknesses was calculated according to the following equation:

$$\Delta f = f_{up} - f_{low}, \quad (4)$$

where f_{up} and f_{low} were the upper and lower frequency limit for $R \leq -10$ dB, respectively.

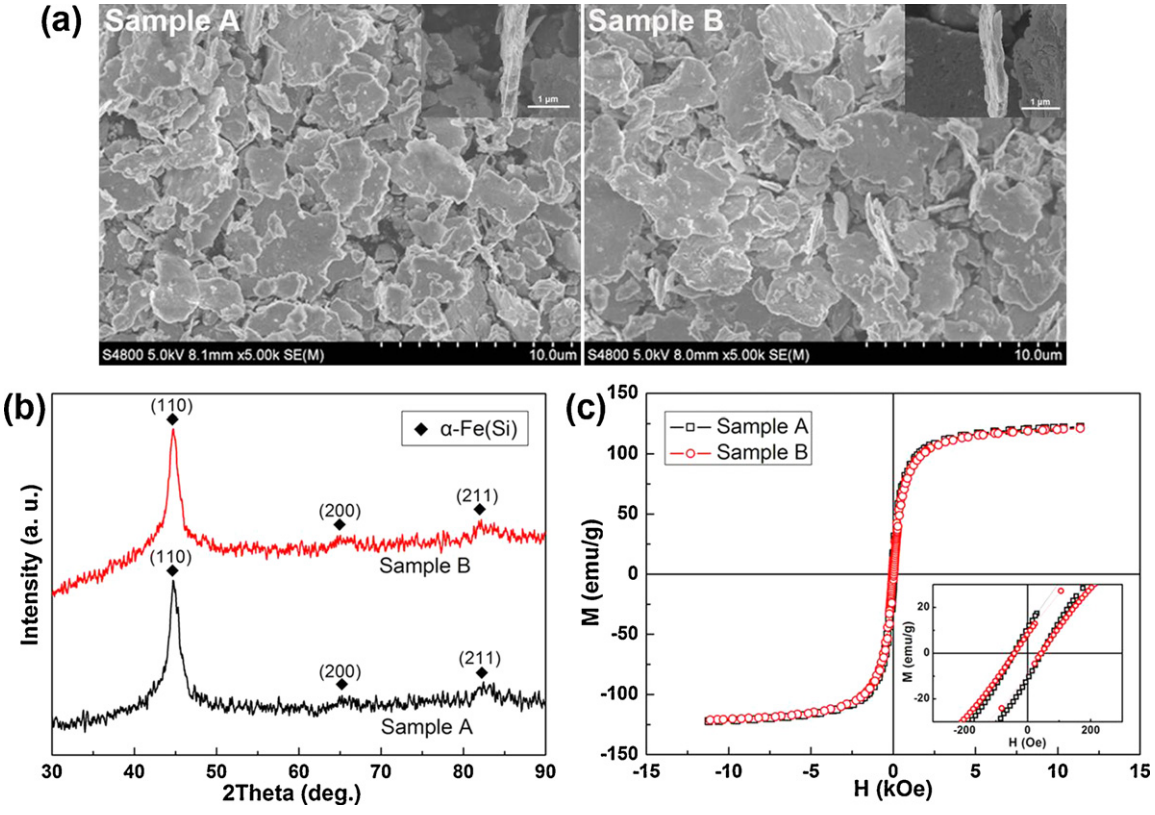

Fig. 2. SEM images (a), XRD patterns (b), and hysteresis loops (c) for Sample A and Sample B. The insets of (a) are the high magnification images of corresponding samples.

3. Results and discussion

3.1. Morphology, structure and static magnetic properties

Fig. 2(a) shows the SEM images of Sample A and Sample B. These pictures demonstrate that Sample A and Sample B have the same morphology and size distribution. They are both the nanoflakes with an average size of 5 μm and a mean thickness of 300 nm (the insets of Fig. 2(a)). Therefore, the aspect ratio is close to 20:1. The smaller thickness of nanoflakes would effectively suppress the eddy current, which is beneficial to increase the permeability in the high frequency range [17]. The high aspect ratio of the nanoflakes makes the easy direction of magnetization located in the plane of the nanoflakes, which makes the nanoflakes achieve bianisotropy for increasing permeability and resonance frequency simultaneously [7,14].

Fig. 2(b) shows the XRD patterns of Sample A and Sample B. The coherence of the diffraction peaks illustrates that Sample B has the same structure with Sample A. The structure of α-Fe(Si) dispersed in an amorphous matrix is obtained from its crystallization process [18]. The average grain size is about 8 nm, which is calculated using the Scherrer formula with the α-Fe (1 0 0) peak. The nanocrystalline state for the nanoflakes is conductive to enhance their soft magnetic properties by decreasing the coercivity [19].

Fig. 2(c) shows the hysteresis loops of Sample A compared with Sample B. The loops indicate the two samples have roughly the same saturation magnetization and coercivity within the measured error range. The values of $4\pi M_s$ and H_c are 11 kG and 42 Oe, respectively.

Fig. 3 presents a TEM picture and XPS survey spectrum of Sample B. It can be seen from Fig. 3(a) that the surface of the nanoflakes is coated with a 10 nm thickness shell. Fig. 3(b) reveals the surface of the nanoflakes (~5 nm) enriched in the element of Oxygen (calibrated by C1s), which demonstrates the nanoflakes can be coated with an oxide-shell by moderate oxidization. The oxide-shell can make the nanoflakes avoid being oxidized further. The thickness of the oxide-shell is about 10 nm, while the thickness of the nanoflake is about 300 nm. Therefore, the volume concentration of the oxide-shell is just below 7%. As a result, the variation of the magnetic properties is just in the range of the instrument's error and can be not obviously detected in the measurement.

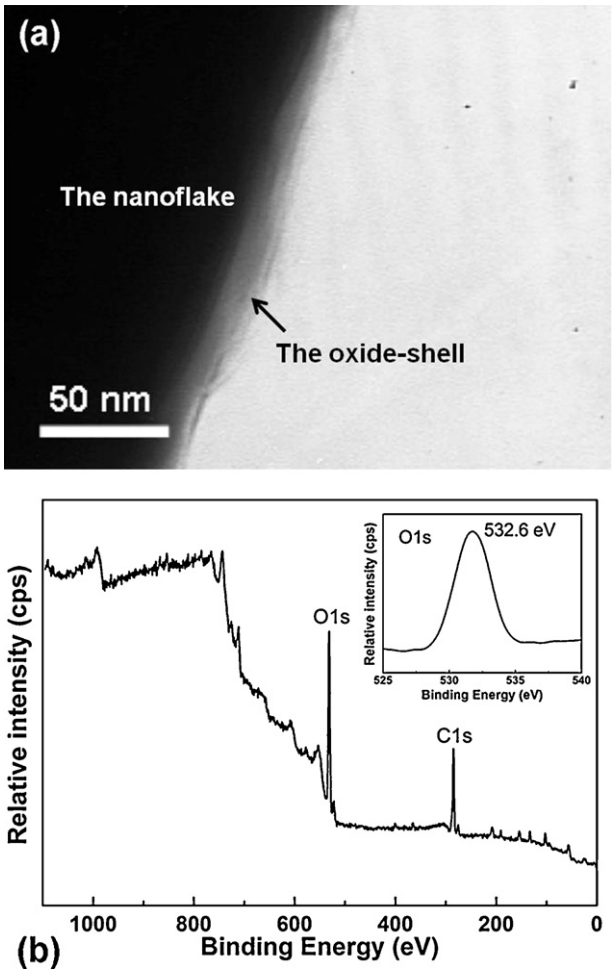

Fig. 3. TEM image (a) and XPS survey spectrum (b) of Sample B. The inset of (b) is the region scan of O1s.

3.2. Dynamic electromagnetic properties

The real part (ε') and imaginary part (ε'') of the permittivity of Composite A, Composite B and Composite C dependent on frequency are shown in Fig. 4(a) and (b), respectively. Compared with Composite B and Composite A, the average value of ε' declines from 70 to 50, while that of ε'' decreases from 40 to 10. The oxide-shell can increase the resistance of the nanoflake and suppress the polarization of its electric charge. As a result, the permittivity of the composites can decrease drastically and match effectively with the permeability. For Composite C, both of the ε' and ε'' are lower than those of Composite B. The average values of ε' and ε'' change from 50 to 40 and from 10 to 5, respectively. As a whole, the ε' and ε'' of the $Fe_{73.5}Cu_1Nb_3Si_{15.5}B_7$ nanoflakes composites are both reduced by moderate oxidization for the nanoflakes and rotational orientation for the composites.

The real part (μ') and imaginary part (μ'') of the permeability of Composite A, Composite B and Composite C dependent on frequency are shown in Fig. 5(a) and (b), respectively. Both of Composite A and Composite B have almost the same spectra of the permeability due to the thin oxide-shell coating on the nanoflakes. For Composite C, both of the μ' and μ'' are higher than those of Composite B. The μ' of Composite C at 0.1 GHz is about 7.0, whereas that of Composite B is only 5.1. The μ'' of Composite C has a maximum value of about 2.3, whereas that of Composite B is about 1.7. As a whole, the μ' and μ'' of the $Fe_{73.5}Cu_1Nb_3Si_{15.5}B_7$ nanoflakes composites remain the same by moderate oxidization for the nanoflakes and increase by rotational orientation for the composites.

3.3. Microwave absorption properties

Fig. 6 shows the bandwidth (Δf) and the minimum reflectivity (R_{min}) of Composite A, Composite B and Composite C over 0.1–18 GHz with various thicknesses from 1.0 to 8.0 mm. The microwave absorption properties of the three composites are summarized in Table 1. It is obvious that Composite C has a higher value of bandwidth and a lower value of minimum reflectivity compared with Composite A and Composite B. The bandwidth of Composite A keeps 0 in the whole thickness range of 1.0–8.0 mm and frequency range of 0.1–18 GHz. Meanwhile, the minimum reflectivity of Composite A is higher than −10 dB in the corresponding thickness and frequency ranges. However, as for Composite B, the bandwidth is more than 0 in the thickness range of 2.0–8.0 mm and its maximum value is about 0.54 GHz at the thickness of 2.6 mm. The minimum reflectivity below −20 dB appears in the thickness range of 4.2–8.0 mm over 0.8–0.9 GHz and its minimum value is about −39.0 dB at the thickness of 6.6 mm and the frequency of 0.8 GHz. Furthermore, for the Composite C, the bandwidth is more than 0 in the thickness range of 1.7–8.0 mm and its maximum value is about 0.96 GHz at the thickness of 2.1 mm. The minimum reflectivity below −20 dB appears in the thickness range of 3.1–6.3 mm

Table 1
Microwave absorption properties of Composite A, Composite B and Composite C in the thickness range of 1.0–8.0 mm and the frequency range of 0.1–18 GHz.

Absorber	$R < -20$ dB		Minimum reflection			Maximum bandwidth	
	t (mm)	f (GHz)	R_{min} (dB)	t_m (mm)	f_m (GHz)	t_0 (mm)	Δf (GHz)
Composite A	–	–	−8.27	7.9	0.35	–	–
Composite B	4.2–8.0	0.63–1.28	−38.2	6.6	0.78	2.6	0.54
Composite C	3.1–6.3	0.85–1.83	−46.4	4.2	1.31	2.1	0.96

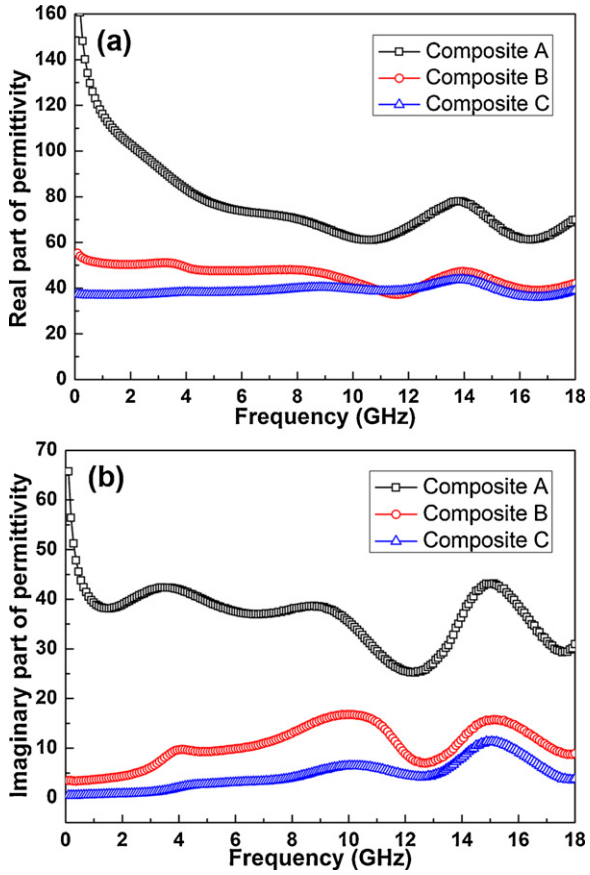

Fig. 4. The real part ε' (a) and imaginary part ε'' (b) of the permittivity of Composite A, Composite B and Composite C in the frequency range of 0.1–18 GHz.

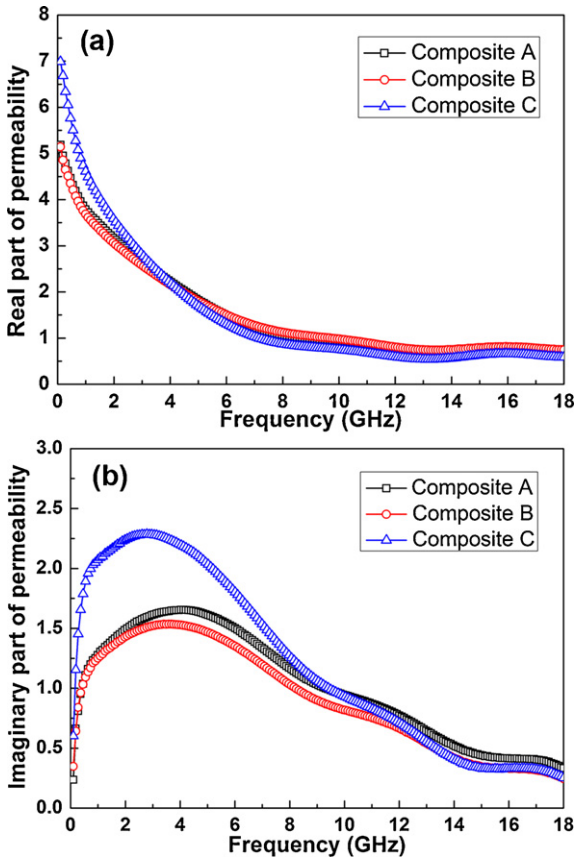

Fig. 5. The real part μ' (a) and imaginary part μ'' (b) of the permeability of Composite A, Composite B and Composite C in the frequency range of 0.1–18 GHz.

over 0.90–1.89 GHz and its minimum value reach −46.4 dB at the thickness of 4.2 mm and the frequency of 1.31 GHz. Summarily, the microwave absorption properties are enhanced by the methods of moderate oxidization for the nanoflakes and rotational orientation for the composites.

The loss tangent and reflectivity of Composite C dependent on frequency at the thicknesses of 3.1, 4.2, 6.3 mm are shown in Fig. 7(a) and (b), respectively. Fig. 7(a) shows that the magnetic loss factor ($\tan\delta_m = \mu''/\mu'$) are higher than the dielectric loss factor ($\tan\delta_e = \varepsilon''/\varepsilon'$) in the frequency range of 0.1–18 GHz, which indicates that the magnetic loss dominate in microwave absorption [20]. So the method of rotational orientation is very effective in improving the microwave absorption properties of the magnetic absorbers. For the absorbers with the thicknesses between 3.1 mm and 6.3 mm, the minimum reflectivity is below −20 dB in the frequency range of 0.85–1.83 GHz. When the thickness is chosen as 4.2 mm, the minimum reflectivity can reach −46.4 dB at 1.31 GHz. The relationship between the matching frequency and the thickness can be expressed by [21]

$$f_m = \frac{c}{4t}\frac{1}{\sqrt{\mu'\varepsilon'}}(1+\tan^2\delta_m)^{-1}, \quad (5)$$

where f_m is the matching frequency, t is the thickness of the absorber. The experimental and calculated results of f_m are compared in Table 2. It is noted that the calculated value (f_m^{cal}) is close to the corresponding experimental result (f_m^{exp}). Therefore, the high permeability and large magnetic loss can reduce the absorber's thickness. The improvement of microwave absorption properties is derived from the electromagnetic matching between the dielectric and magnetic losses [22], which are the results of moderate surface oxidization for the nanoflakes and rotational orientation for the composites.

Table 2
Comparison between the experimental and calculated matching frequency in the thicknesses of 3.1, 4.2, 6.3 mm.

t_m (mm)	3.1	4.2	6.3
f_m^{exp} (GHz)	1.83	1.31	0.85
f_m^{cal} (GHz)	2.01	1.40	0.88

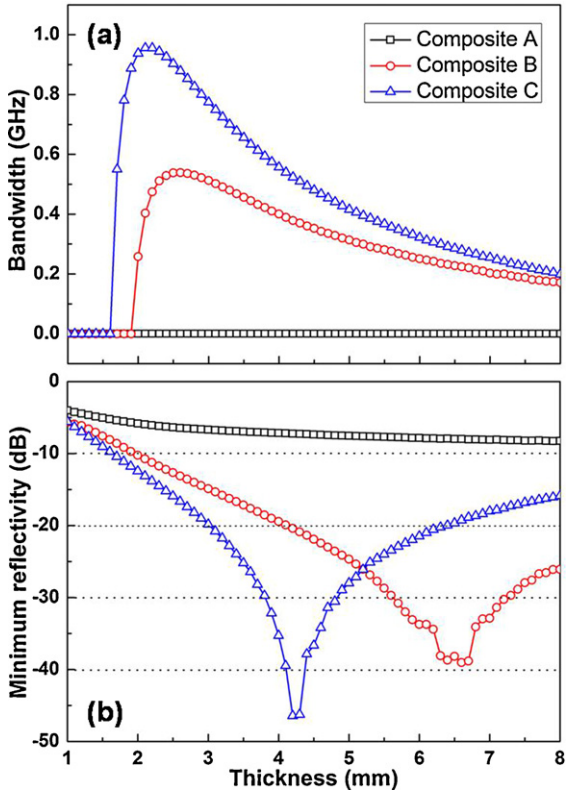

Fig. 6. Bandwidth Δf (a) and minimum reflectivity R_{min} (b) of Composite A, Composite B and Composite C with various thicknesses in the frequency range of 0.1–18 GHz.

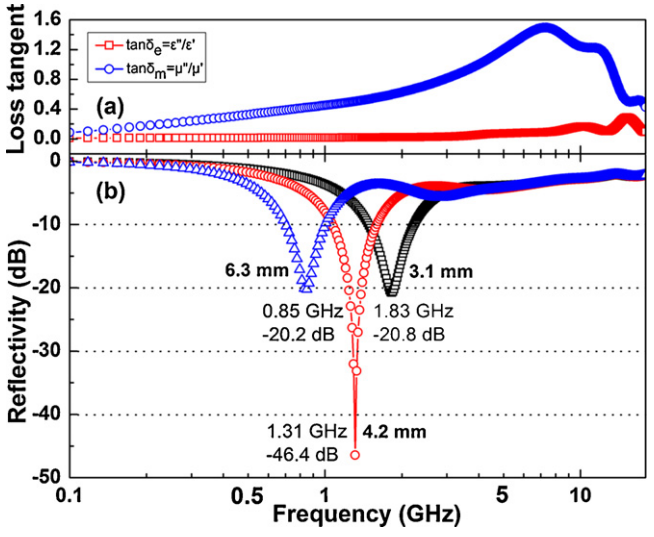

Fig. 7. (a) The dielectric loss factor $\tan\theta_e$ and magnetic loss factor $\tan\theta_m$ of Composite C in the frequency range of 0.1–18 GHz. (b) The reflectivity R of Composite C dependent on frequency at thicknesses of 3.1, 4.2, 6.3 mm.

4. Conclusions

In this paper, $Fe_{73.5}Cu_1Nb_3Si_{15.5}B_7$ nanoflakes were fabricated by ball milling the annealed ribbons, and their microwave absorption properties were improved by moderate surface oxidization and rotational orientation in composites. The lower permittivity was obtained for the nanoflakes after moderate oxidization, while higher permeability was obtained for the nanoflakes composite with rotational orientation. The minimum reflectivity for the absorbers of oriented composites with 35 vol% the oxide-coated nanoflakes could reach −46.4 dB at 1.31 GHz with the thickness of 4.2 mm. The enhanced microwave absorption properties demonstrate the availability of our oxidization and orientation methods in this work.

Acknowledgment

This work was supported by the National Natural Science Foundation of China under Grant no. 10774061.

References

[1] C. Wang, R.T. Lv, Z.H. Huang, F.Y. Kang, J.L. Gua, J. Alloys Compd. 509 (2011) 494–498.
[2] Y. Yang, C.L. Xu, Y.X. Xia, T. Wang, F.S. Li, J. Alloys Compd. 493 (2010) 549–552.
[3] L.D. Liu, Y.P. Duan, S.H. Liu, L.Y. Chen, J.B. Guo, J. Magn. Magn. Mater. 322 (2010) 1736–1740.
[4] S.J. Yan, L. Zhen, C.Y. Xu, J.T. Jiang, W.Z. Shao, J. Phys. D: Appl. Phys. 43 (2010) 245003.
[5] Z. Han, D. Li, M. Tong, X. Wei, R. Skomski, W. Liu, Z.D. Zhang, D.J. Sellmyer, J. Appl. Phys. 107 (2010) 09A929.
[6] Y.K. Lee, Yoon B. Kim, K.K. Jee, G.B. Choi, Phys. Status Solidi (a) 204 (2007) 4100–4103.
[7] D.S. Xue, F.S. Li, X.L. Fan, F.S. Wen, Chin. Phys. Lett. 25 (2008) 4120–4123.
[8] Z.W. Li, L.F. Chen, Y.P. Wu, C.K. Ong, J. Appl. Phys. 96 (2004) 534.
[9] X. Wang, R. Gong, H. Luo, Z. Feng, J. Alloys Compd. 480 (2009) 761–764.
[10] T.D. Zhou, J.K. Tang, Z.Y. Wang, J. Magn. Magn. Mater. 322 (2010) 2589–2592.
[11] P.H. Zhou, J.L. Xie, Y.Q. Liu, L.J. Deng, J. Magn. Magn. Mater. 320 (2008) 3390–3393.
[12] B.S. Zhang, G. Lu, Y. Feng, J. Xiong, H.X. Lu, J. Magn. Magn. Mater. 299 (2006) 205–210.
[13] L.G. Yan, J.B. Wang, X.H. Han, Y. Ren, Q.F. Liu, F.S. Li, Nanotechnology 21 (2010) 095708.
[14] W.F. Yang, L. Qiao, J.Q. Wei, Z.Q. Zhang, T. Wang, F.S. Li, J. Appl. Phys. 107 (2010) 033913.
[15] S.S. Kim, S.B. Jo, K.I. Gueon, K.K. Choi, J.M. Kim, K.S. Churn, IEEE Trans. Magn. 27 (1991) 5462–5464.
[16] Z.W. Li, G.Q. Lin, L.B. Kong, IEEE Trans. Magn. 44 (2008) 2255–2261.
[17] S. Sugimoto, T. Maeda, D. Book, T. Kagotani, K. Inomata, M. Homma, H. Ota, Y. Houjou, R. Sato, J. Alloys Compd. 330 (2002) 301–306.
[18] A. Gavrilović, D.M. Minić, L.D. Rafailović, P. Angerer, J. Wosik, A. Maričić, D.M. Minić, J. Alloys Compd. 504 (2010) 462–467.
[19] G. Herzer, J. Magn. Magn. Mater. 157/158 (1996) 133–136.
[20] X.G. Liu, Z.Q. Ou, D.Y. Geng, Z. Han, Z.G. Xie, Z.D. Zhang, J. Phys. D: Appl. Phys. 42 (2009) 155004.
[21] K.M. Lim, M.C. Kim, K.A. Lee, C.G. Park, IEEE Trans. Magn. 39 (2003) 1836–1841.
[22] X.F. Zhang, X.L. Dong, H. Huang, Y.Y. Liu, B. Lv, J.P. Lei, C.J. Choi, J. Phys. D: Appl. Phys. 40 (2007) 5383.